W&T samenwerking met Centraal - en Oost - Europa
Beurzen aan onderzoekers (selectieronde 2011)

BELSPO FELLOWSHIP

(2011-2012)

Spin-charge phenomena in graphene and semiconductor nanostructures

RESEARCH REPORT

(Final-report)

Researcher: **Dr. S. M. Badalyan**
Promotor: **Prof. F. M. Peeters**

Condensed Matter Theory, Department of Physics
University of Antwerp, Groenenborgerlaan 171
B-2020 Antwerpen, Belgium

Antwerpen – 2012

Abstract

During the fellowship we have studied six different aspects of spin/charge scattering phenomena in individual and double layer structures of graphene and conventional semiconductors. Specifically, we have predicted a strong effect of the *inhomogeneity of dielectric background* on the plasmon modes in graphene double layer structures. It has been shown that the energies of in-phase and out-of-phase plasmon modes are determined by the different values of the dielectric permittivity, which results in new features of the optical and acoustical plasmon dispersions that can be probed in frictional drag measurements, in inelastic light scattering and electron energy-loss spectroscopy. Next, we have investigated the drag of massless fermions in graphene double-layer structures in a wide rage of temperatures and interlayer separations. It has been shown that the inhomogeneity of the dielectric background in such graphene structures, for experimentally relevant system parameters, results in a significant *enhancement of the drag* resistivity. Moreover, at intermediate temperatures the dynamical screening via plasmon-mediated drag enhances the drag resistivity and results in an upturn in its behavior at large interlayer separations. We have found that in a range of interlayer separations, corresponding to the strong-to-weak crossover coupling of graphene layers, the drag resistivity decreases approximately quadratically with the interlayer spacing. This dependence weakens with a decrease of the spacing while for larger separations we recover the cubic (quartic) dependence at intermediate (low) temperatures. Thus, our calculations provide an understanding of the Coulomb drag temperature and interlayer spacing behavior. The new enhancement mechanisms of drag proposed are to get rid the current discrepancy between theory and experiment. In other field of electron-phonon interaction we have calculated the *fine structure* of the Dirac energy spectrum in graphene, induced by electron-optical phonon coupling and have derived a new dispersion equation that corresponds to an electron-phonon *bound state*. It has been predicted that the singular vertex corrections beyond perturbation theory increase strongly the scale of the electron-phonon binding energy and that the enhancement obtained can be probed using angle-resolved spectroscopy. Furthermore, in our recent paper we have investigated the spectrum of electron-phonon complexes in a monolayer graphene in the presence of a perpendicular quantizing magnetic field. Our findings beyond perturbation theory show that the true electronic spectrum above and below the phonon emission threshold is completely governed by new branches of the spectrum, corresponding to bound states of an electron and an optical phonon with an enhanced binding energy scale. The obtained bound states manifest themselves in the light absorption spectrum as an *asymmetric doublet* around the threshold frequency. In another work we have proposed a new method for the *generation of spin currents* from the Coulomb-Rashba type spin-orbit coupling in semiconductor bilayers. The predicted new effect of *spin drag* consists of spin accumulation across one layer when an electric current flowing along the other layer. It arises from the combined action of spin-orbit and interlayer Coulomb interactions. The induced spin accumulation is observable in optical rotation experiments. In our latest work we have studied the momentum relaxation of Dirac fermions due to scattering from the *piezoelectric* acoustical (PA) phonons, propagating on the surface of GaAs, versus the deformation acoustical phonons of graphene. We have shown that electron-PA phonon scattering is the dominant mechanism, limiting the mobility in graphene at relatively low carrier densities. Moreover, PA phonons change *qualitatively* the mobility dependence on the density of electrons and on the lattice temperature, respectively, in the regimes of high and low temperatures.

Keywords

Graphene, semiconductor nanostructures, many-spin/charge phenomena, electron-phonon interaction, quantizing magnetic field, spin-orbit interaction, double-layer electronic systems, cyclotron-phonon resonance, carrier mobility and momentum relaxation in graphene

List of publications resulting from the fellowship

Papers in refereed journals and preprints

- S. H. Zhang, W. Xu, **S. M. Badalyan**, and F. M. Peeters, Piezoelectric surface acoustical phonon limited mobility of electrons in graphene on a GaAs substrate, submitted for publication in Physical Review Letters, arXiv:**1211.6280**.
- J. Zhu, **S. M. Badalyan** and F. Peeters, Electron-phonon bound states in graphene in a perpendicular magnetic field, in press in Physical Review Letters, arXiv: **1206.5107**.
- **S. M. Badalyan** and F. Peeters, Enhancement of Coulomb drag in double-layer graphene structures by plasmons and dielectric background inhomogeneity, Phys. Rev. B **86**, 121405(R) (2012).
- **S. M. Badalyan** and F. Peeters, Electron-phonon bound states in graphene, Phys. Rev. B **85**, 205453 (2012).
- **S. M. Badalyan** and F. Peeters, Effect of nonhomogeneous dielectric background on the plasmon modes in graphene double-layer structures at finite temperatures, Phys. Rev. B **85**, 195444 (2012).
- M. M. Glazov, M. A. Semina, **S. M. Badalyan**, and G. Vignale, Spin-current generation from Coulomb-Rashba interaction in semiconductor bilayers, Phys. Rev. B **84**, 033305 (2011).

Oral presentations in scientific meetings and seminar talks

- S. M. Badalyan, Spin Coulomb drag, *Condensed Matter Theory Seminar, the Department of Physics,* Antwerp University, October 2011, Antwerp, **Belgium**
- S. M. Badalyan, Plasmon modes in graphene double-layer structures at finite temperatures, invited talk at the *Meeting of the Belgian Physical Society*, May 30, 2012 Brussels, **Belgium**.
- S. M. Badalyan, Effect of nonhomogeneous dielectric background on the plasmon modes in graphene double-layer structures, *March Meeting of the American Physical Society,* February 27—March 2, 2012 Boston, **USA**

Contributions (poster) to academic conferences

- M. M. Glazov, M. A. Semina, **S. M. Badalyan**, and G. Vignale, Spin accumulation from electron-electron scattering in semiconductor bilayers, *31st International Conference on the Physics of Semiconductors*, July 29th—August 3rd 2012, Zurich, **Switzerland**.
- **S. M. Badalyan** and F. Peeters, Electron-phonon bound states in graphene, *31st International Conference on the Physics of Semiconductors*, July 29th—August 3rd 2012, Zurich, **Switzerland**.

- J. Zhu, **S. M. Badalyan** and F. Peeters, Electron-phonon bound states in graphene in a perpendicular magnetic field, *Meeting of the Belgian Physical Society,* May 30, 2012 Brussels, **Belgium**.

Collaborations during the fellowship

F. M. Peeters
Head of the CMT group
Department of Physics, University of Antwerp, Antwerp, **Belgium**

J. Zhu
Postdoc in the CMT group
Department of Physics, University of Antwerp, Antwerp, **Belgium**

M. M. Glazov
Dr., Sci. researcher
Ioffe Physical-Technical Institute of the Russian Academy of Sciences, St. Petersburg, **Russia**

M. A. Semina
Researcher
Ioffe Physical-Technical Institute of the Russian Academy of Sciences, St. Petersburg, **Russia**

G. Vignale
Professor
Department of Physics and Astronomy, University of Missouri, Columbia, Missouri 65211, **USA**

S. H. Zhang
PhD student
Visitor at the CMT group, Department of Physics, University of Antwerp, **Belgium,**
Key Laboratory of Materials Physics, Institute of Solid State Physics, Chinese Academy of Sciences, Hefei 230031, **China**

W. Xu
Professor
Key Laboratory of Materials Physics, Institute of Solid State Physics, Chinese Academy of Sciences, Hefei 230031, **China**

Other professional activities

Active referee for Physical Review Letters, Physical Review B, Europhysics Letters, Journal of Applied Physics, Physica Status Solidi, Physica B.

Member of the PhD jury of M. Barbier at the University of Antwerp.

Accomplishments of the fellowship and future work

During the fellowship new important issues, which have been closely related to the planned objectives of our project, have appeared. Accordingly in some parts, we have partially modified our initial program, giving priority to the investigation of those problems.

The accomplishments of the fellowship as described below are at the frontier of an exciting area of modern condensed matter physics in low dimensions and provide

substantial advancement in the field of semiconductor nanostructures and graphene physics.

Dr. Badalyan was offered an extension of his postdoc position and will continue his research in the Condensed Matter Theory group during 2013. Several aspects of the ongoing research will be continued and in the research of graphene will be pursued.

Results of the research

Spin-charge phenomena in graphene and semiconductor nanostructures

I. Introduction

Low dimensional electron systems [1] continue to drive both fundamental condensed matter physics and the development of semiconductor technology applications. Recently exceptionally dynamic fields of semiconductor spintronics [2-5] and graphene physics [6-9] have emerged with a promise of bringing completely new device functionalities and of extending the scientific and technological frontiers of electronic industry. The feasibility of inventing such revolutionary spintronic devices is based particularly on the potential of integrating the unique storage capacity of magnetic memory with the outstanding computing power of semiconductor logic. Possibilities are additionally enhanced by the long-lasting quantum coherence of spin states in semiconductor nanostructures. Crucial requirements for such device structures are the existence of a robust population of spin-polarized carriers, their selective, local manipulation and control by means of spin currents. Recent discovery of graphene [7,8], which is a monolayer of carbon atoms with a unique conical gapless bandstructure, provides a new rich area for fundamental investigations with a great potential for new generation electronics [9,10]. Charge and (pseudo)spin carriers in graphene are Dirac-like massless, chiral fermions, which provide a unique two-dimensional electron system with new interaction phenomena that can critically influence the electronic properties of graphene and its future device applications. For the realization of the huge potential of semiconductor spintronics and graphene physics, the theoretical and practical understanding of transport, dynamical response, and relaxation processes of (pseudo)spin-charge carriers becomes urgent and extremely important, to which, as discussed below, we strive to contribute.

For last decade the vigorous research efforts of the *fellow* have been mainly aimed at understanding the carrier transport, relaxation and optical properties in low dimensional

electron systems in semiconductor nanostructures and graphene. Particularly, for last several years in collaboration with several theoretical groups the fellow has predicted such novel phenomena as the beating of Friedel oscillations [11] and the spin Hall drag [12,13]; has provided a deeper understanding of the experimental observations [14] beyond the random phase approximation that proves the existence of spin Coulomb drag [15]; he has developed a new method for calculation of the carrier polarizability in the presence of the spin-orbit coupling [16] and has presented new exact solutions to the problem of spin edge states [17,18].

During the present fellowship, the *fellow* in collaboration with the *host professor* F. M. Peeters has investigated many-body electron-phonon [19-27] and electron-electron scattering phenomena in an individual [27-35] and double-layer graphene [36-45] structures in zero and finite magnetic fields. Specifically, we have calculated the effect of dielectric background inhomogeneity on the plasmon spectrum in graphene double layer structures as well as have predicted the existence of new electron-phonon complexes in individual graphene layers in zero and a quantizing magnetic field. We have studied Coulomb drag in graphene [46-54] and put forward its two enhancement mechanisms by plasmons and dielectric background inhomogeneity. In collaboration with theorists from the Columbia-Missouri University, USA and from the Ioffe Physical-Technical Institute, Russia, the *fellow* has studied the spin-orbit interaction in the electric field of interlayer Coulomb interaction in double-layer semiconductor heterostructures and the generation of a spin current in one layer when a charge current is driven in the other.

II. Overview of the obtained results and conclusions

Effect of nonhomogenous dielectric background on the plasmon modes in graphene double-layer structures

In this work we have predicted a strong effect of the inhomogeneity of dielectric background on the plasmon modes in graphene double layer structures (*cf.* Fig. 1(left)). The Poisson equation for a three layer dielectric medium has been solved exactly and the effective dielectric function of graphene double layer structures has been obtained. We have found that the effective dielectric function shows a finite spatial dispersion due to its dependence on the bosonic momentum q (*cf.* Fig. 1(right)). This results in an additional momentum dependence of the bare intra- and interlayer Coulomb interactions—an effect of the order of interlayer interaction itself. In its turn this new momentum dependence

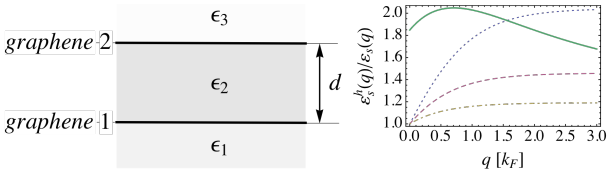

FIG. 1. Left: A graphene double-layer system (GDLS) immersed in a three-layer nonhomogeneous dielectric medium. Right: The solid curve corresponds to the ratio of the double-layer static screening functions $\varepsilon_{hs}(q)$ to $\varepsilon_s(q)$, which are calculated, respectively, in GDLS with a homogeneous average permittivity and in GDLS with a nonhomogeneous dielectric background, corresponding to the three-layered medium of the left figure. It is seen that $\varepsilon_s(q)$ differs essentially from the screening function $\varepsilon_{hs}(q)$.

induces strong modifications in the energy dispersions of the plasmon modes in graphene double layer structures. It has been shown that the energies of in-phase optical and out-of-phase acoustical plasmon modes are determined by different values of the effective dielectric permittivity. The effect of dielectric inhomogeneity is found the largest for samples with $d\sim10$ nm and for finite values of $q\sim k_F$. Our approach allows us to find the plasmon dispersions at finite temperatures and to treat additionally two new aspects. First, we have shown that temperature has a strong effect on the acoustical plasmon mode in a completely unbalanced system—the acoustical mode becomes separated from the top of the electron-hole continuum and this creates a possibility to observe it. Second, we have found that the effect of dielectric inhomogeneity at finite temperatures remains as strong as at zero temperature (*cf.* Fig. 2). These predicted new features of the plasmon dispersions can be probed in frictional drag measurements, in inelastic light scattering and electron energy-loss spectroscopy.

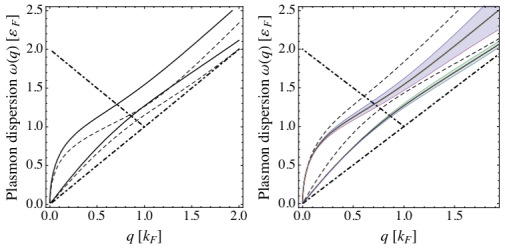

FIG. 2. (left) Temperature effect on the in-phase and out-of-phase plasmon modes in GDLS with nonhomogenous dielectric background. The dashed and solid lines correspond to $T = 0.1T_F$ and $T=T_F$. (right) The effect of nonhomogenous dielectric background on the plasmon dispersions in GDLS at $T = T_F$. The solid (dashed) curves are calculated for the plasmon modes in GDLS with nonhomogenous (homogenous) dielectric background. The plasmon dispersions are shown in the exactly balanced GDLS with the inlayer density, $n_1 = n_2 = 10^{12}$ cm^{-2} and for the interlayer spacing $d =$ 10 nm. The shaded areas represent the broadening of the energy dispersions of respective plasmon modes.

Enhancement of Coulomb drag in graphene double-layer structures by plasmons and dielectric background inhomogeneity

In another work we have calculated the Coulomb drag resistivity in graphene double-layer structures (GDLS) in a wide rage of temperatures, T, and of interlayer separations using the finite-T polarizability and the finite-T nonlinear susceptibility for individual graphene layers. We have focused on three main questions. First, we have investigated the effect of the dielectric inhomogeneity of the GDLS surrounding environment on the drag and have shown that Coulomb drag in GDLS immersed in a three

layer nonhomogeneous dielectric medium is significantly larger than that calculated for the respective averaged homogenous background (*cf.* Fig. 3(left)). Then, we have calculated the contribution to the drag made by double-layer optical and acoustical plasmon modes via the dynamical screening. We have found that at intermediate temperatures the dynamical screening results in the plasmon enhancement of drag, which for the interlayer spacing d=30 nm shows an upturn in the drag resistivity at

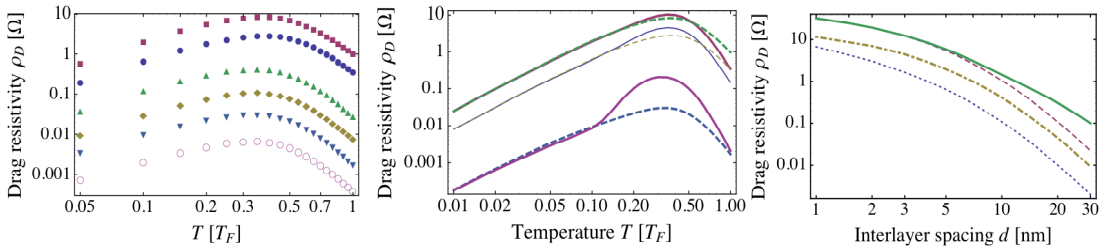

FIG. 3. (left) The effect of the dielectric background inhomogeneity on the Coulomb drag in GDLSs. The top pair of symbols shows the log-log plot of the drag resistivity as a function of scaled temperature in GDLSs with d = 5 nm interlayer spacing, immersed in a nonhomogeneous (the upper set) and homogeneous (the lower set) dielectric background corresponding to the GDLS in Fig. 1(left). The two other pairs of data sets in the middle and bottom of the figure correspond, respectively, to d = 15 and 30 nm interlayer spacing. All curves have been calculated within the static screening approximation. (mid) Plasmon enhancement of Coulomb drag of massless fermions in GDLSs. The top and bottom bold curves are log-log plots of the drag resistivity vs scaled temperature for d = 5 and d = 30 nm interlayer spacing, respectively. The solid curves correspond to calculations using the finite temperature exact polarization and nonlinear response functions while the dashed curves are calculated within the static screening approximation. The parameters are the same as in Fig. 1 for GDLSs with a nonhomogeneous dielectric background. The thin curves correspond to the calculations for d = 5 nm in GDLSs with a homogeneous dielectric background. (right) The log-log plot of the drag resistivity as a function of the interlayer spacing d for $T = 0.2T_F$ (the solid and dashed curves) and for $T = 0.1T_F$ (the dotted-dashed and dotted curves). The solid curve corresponds to calculations using the finite temperature exact polarization and nonlinear response functions, and the other curves are based on the static screening approximation. The dotted curve is calculated for GDLSs with a homogeneous dielectric background, and the other curves for GDLSs with a nonhomogeneous dielectric background.

approximately $0.15T_F$ (*cf.* Fig. 3(mid)). Next, we have studied the dependence of the drag rate on the interlayer spacing. It has been found that the drag resistivity decreases with the interlayer spacing approximately quadratically for interlayer separations, corresponding to the strong-to-weak interlayer coupling crossover. This dependence increases (decreases) with an increase (decrease) of the interlayer spacing (*cf.* Fig. 3(right)).

The Coulomb drag is an outstanding problem because of its critical importance for studying interaction phenomena. Our calculations incorporate all the present-day advancements in the theory of Coulomb drag and provide an understanding of its temperature and interlayer spacing behavior. The current experimental findings [41] show that the measured drag exceeds by a factor of 3 the previously calculated drag values by other theoretical groups. We have put forward two new enhancement mechanisms of drag in graphene, which should influence the understanding of

experimentalists and theorist who investigate double-layer graphene structures and should get rid of the above discrepancy between theory and experiment.

Electron-optical phonon bound states in graphene

In this paper we have studied the fine structure of the electronic spectrum in graphene induced by electron-phonon coupling in the neighborhood of the optical phonon emission threshold. In this range of energies the lowest order electron mass operator and its higher order vertex corrections are singular. Hence usual perturbation theory is inapplicable that complicates the problem. We have developed a threshold approximation in graphene and obtained the spectrum by solving the Dyson equation for the electron Green function coupled with the Dyson-type equation for the exact electron-phonon vertex part. It allows us to sum an infinity series of ladder-type diagrams and to derive a new dispersion relation for the quasiparticle energy

$$\varepsilon - v_F(p - p_F) = -\omega_0 \frac{g \ln \frac{\varepsilon_F}{\omega_0 - \varepsilon}}{1 - g \ln \frac{\varepsilon_F}{\omega_0 - \varepsilon}}$$

where ε and p are the quasiparticle energy and momentum, ε_F and p_F the Fermi energy and momentum, ω_0 the phonon frequency, and g is the electron-phonon coupling constant. The dispersion equation determines new properties of the electron-phonon compound states. A qualitative new feature of the spectrum is that it does not asymptotically tend to the

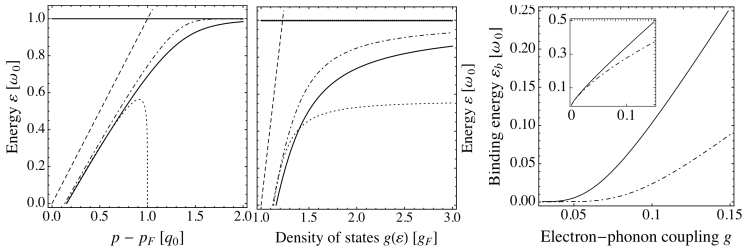

FIG. 4. (right) The energy spectrum of the electron-optical phonon quasiparticle for the electron density n = 5.6 10^{13} cm^{-2}. The horizontal solid line is the phonon emission threshold. (mid) The corresponding density of states $g(\varepsilon)$ of the quasiparticle in units of $g_F = 2k_F/\pi v_F$. (left) The electron-phonon binding energy versus the bare coupling g for $p - p_F = 1.5q_0$. Inset shows the binding energy of the hybrid states at the resonance $p - p_F = q_0$. In all figures the dashed lines represent the bare Dirac fermions, the dotted and dot-dashed curves are calculated, respectively, within the Rayleigh-Schroedinger and Wigner-Brillouin perturbative approaches. The solid curve is obtained within the present theory, taking into account the singular vertex corrections beyond perturbation theory.

phonon energy and remains always below it at the small but finite distance (*cf.* Fig. 4). Hence in the immediate neighborhood below the phonon threshold the spectrum corresponds to an electron-phonon bound state. For large values of the wave vector the binding energy depends exponentially on the bare coupling and for experimentally accessible values of the bare coupling it will be measurable only in clean samples with

high values of the mobility. Furthermore, for not very large wave vectors we have found that the singular vertex corrections enhance strongly the effective electron-phonon coupling. The binding energy has a new scale, which is more than a factor of 5 larger than that obtained within the previous perturbative approaches (*cf.* Fig. 4(right)). This enhanced coupling effect will manifest itself in angle-resolved measurements with the resolution smaller than the binding energy as a significant deviation from the linear Dirac spectrum at frequencies below the phonon energy and wave vectors larger than its resonance value. The predicted fine structure of the spectrum is a new effect in graphene physics, which can have optical and electronic applications in graphene device structures.

Electron-phonon bound states in graphene in a perpendicular quantizing magnetic field

Lately we have studied the spectrum of electron-phonon structures in monolayer graphene, exposed to a perpendicular quantizing magnetic field. The Landau quantization in graphene (*cf.* Fig. 5(left)) is currently well established both in theory and experiment. Recently it was proposed theoretically [20] that in addition to the Landau levels, new discrete states exist in the graphene spectrum at the energies above and below of the bare Landau levels on the distance of the phonon energy. This concept is based on perturbation theory and assumes that electronic transitions involve optical phonons, which exist but do not interact with electrons.

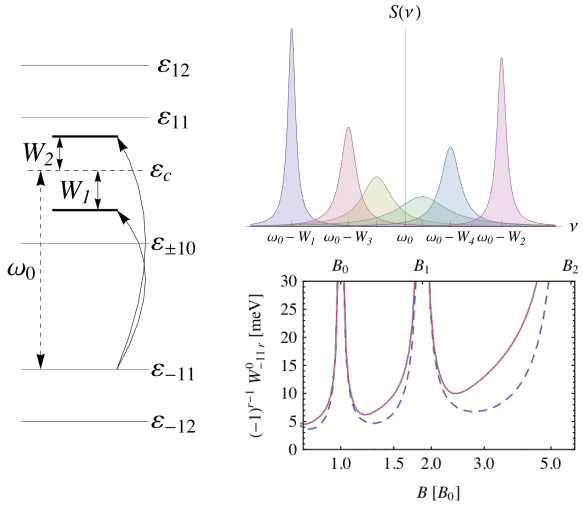

FIG. 5. (left) The electron energy spectrum in graphene, exposed to a perpendicular quantizing magnetic field. The dashed line represents the phonon-emission threshold energy. In contrast to the prediction from Ref. [20], no state corresponds exactly to the threshold energy. Instead, the true spectrum includes a sequence of electron-phonon bound states, which coagulates to the threshold. The most distant bound states with the binding energies $W_{1,\,2}$ of opposite signs are shown in a larger scale by the bold, solid lines below and above the threshold. (top right) Schematic diagram of the absorption spectrum in graphene. The cyclotron-phonon resonance is governed by the peaks corresponding to the electron-phonon bound states, which constitute an asymmetric doublet around the phonon-emission threshold. (bottom right) The binding energies $W^0_{\rm nr}$ for the bound states, which refer to the threshold for the negative Landau level with $n = 1$. The solid and dashed curves correspond to the $r = 1$ and 2 bound states, which are most distant from the threshold.

In the present work we have employed a new method beyond perturbation theory for the calculation of the graphene electronic spectrum in a quantizing magnetic field. We have shown that even for small electron-

phonon coupling, the states predicted in Ref. 20 do not exist, instead, the true spectrum includes a sequence of electron-phonon bound states, which coagulate to the threshold of optical phonon emission above and below it. The bound states obtained (*cf.* Fig. 5(bottom right)) manifest themselves in the light absorption spectrum as an asymmetric doublet (*cf.* Fig. 5(top right)) around the threshold frequency. The prediction of the fine structure of the cyclotron-phonon resonance governed by these new branches of the electronic spectrum should critically influence magneto-optical properties of graphene.

Spin-current generation from Coulomb-Rashba interaction in semiconductor bilayers

In this paper we have uncovered a novel effect in semiconductor bilayers: the electron spin accumulation, generated by an interplay of the regular spin-orbit coupling and the spin-orbit coupling in the electric field of interlayer interaction, induced by carrier density fluctuations. This effect allows a "non-local" spin injection from one layer into another (*cf.* Fig. 6). The spin, along with the charge, is a fundamental property of electrons and the problem of the current conversion between these different degrees of freedom is of high importance for device applications and for the development of fundamental physics.

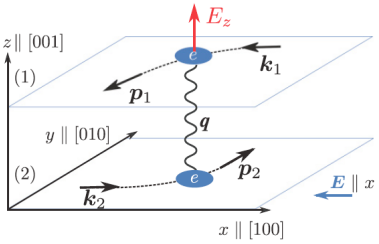

FIG. 6. Scheme of the device under study: An electric field $\boldsymbol{E}$ is applied to the active layer (2), and a spin current is generated in the passive layer (1). Blue circles depict electrons, and the wavy line shows the interlayer Coulomb interaction. Arrows marked $\boldsymbol{k}_1$,$\boldsymbol{k}_2$ and $\boldsymbol{p}_1$, $\boldsymbol{p}_2$ are the wave vectors in the initial and final states. The vertical arrow emphasizes the relevant component of the interlayer Coulomb field.

We have shown that electrons in double-layer semiconductor heterostructures experience a special type of spin-orbit interaction that arises in each layer from the perpendicular component

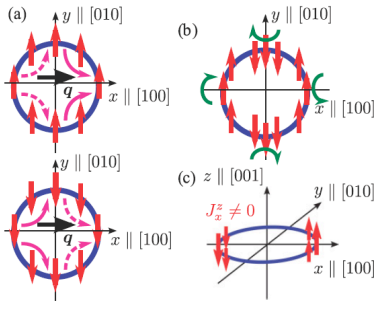

FIG. 7. Schematic of the spin-current generation in the passive layer. The circle is the Fermi surface, and the arrows are the electron spins. Panel (a) shows the scattering stage of the process: The top part shows electrons with spin parallel to the y axis, and the bottom part shows electrons with spin antiparallel to the y axis. The arrows show the spin-dependent scattering process: Solid arrows indicate the stronger transitions, having $k_x + p_x > 0$ for $s_y > 0$ and $k_x + p_x < 0$ for $s_y < 0$, while dashed arrows indicate the weaker transitions. Scattering processes that increase the x component of the wave vector (i.e., with $q_x > 0$) dominate due to the current flowing in the active layer. (b) Precession stage of the process. The resulting spin distribution after the scattering contains second angular harmonics. Green arrows demonstrate the spin precession caused by the Dresselhaus field. Electron spins with opposite wave vectors precess in opposite directions. The resulting dipolar distribution of electron spins is presented in panel (c).

of the Coulomb electric field created by electron-density fluctuations in the *other* layer. This new interaction, acting in combination with the usual spin-orbit interaction, can

generate a spin current in one layer when a usual charge current is driven in the other. This effect is distinct symmetrywise from our earlier prediction of the spin-Hall drag [12] and the spin current we have obtained in the present paper is not, in general, perpendicular to the drive current. Thus, we have described a new coupling mechanism (*cf.* Fig. 7), due to partly interlayer Coulomb and partly spin-orbit interactions, through which a spin current can be injected, or a spin accumulation can be induced, in an electron layer by a regular electric current flowing in an adjacent layer. The coupling can play a role in the design of circuits in which an electric current must be converted into a spin current and vice versa.

Piezoelectric surface acoustical phonon limited mobility of electrons in graphene on a GaAs substrate

In our latest paper we have studied the mobility of Dirac fermions in monolayer graphene on a GaAs substrate, limited by the combined action of the extrinsic potential of piezoelectric surface acoustical phonons of GaAs and of the intrinsic deformation potential of acoustical phonons in graphene. Recently, graphene device structures on GaAs substrates [21,22] have been fabricated and studied with the intention for high-quality graphene electronics. Because of the superior surface quality, high purity, and strong hydrophilicity of GaAs, electron-phonon scattering processes can be a decisive factor in limiting the mobility of Dirac fermions. On the other hand, the piezoelectric GaAs substrate can serve as a powerful tool for probing electronic properties of graphene by means of remote piezoelectric surface acoustical phonons.

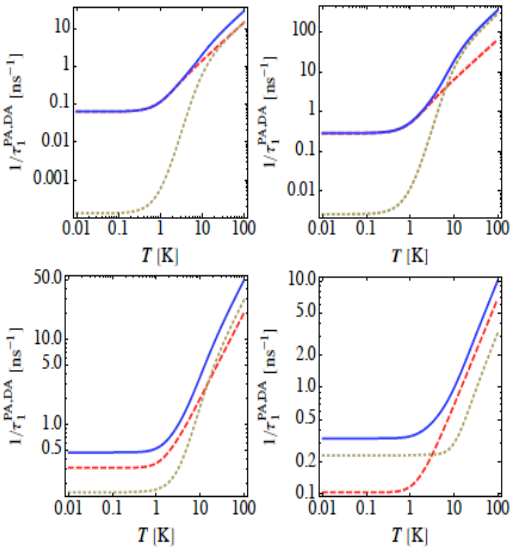

FIG. 8. The electron momentum relaxation rate as a function of temperature for different values of the electron energy and density. The dashed and dotted lines correspond to the extrinsic PA and intrinsic DA phonon scattering mechanisms. The solid curve is the total rate. Four different situations are presented: (top, left) ε-ε_F = 3 K and n = 0.5 10^{12} cm^{-2}, (top, right) ε-ε_F = 3 K and n = 10^{13} cm^{-2}, (bottom, left) ε-ε_F = 15 K and n = 10^{12} cm^{-2}, and (bottom, right) ε-ε_F = 30 K and n = 10^{11} cm^{-2}.

We have calculated the momentum relaxation rate of Dirac fermions and have found the contribution to the mobility made by such extrinsic piezoelectric acoustical (PA) phonons, propagating on the surface of GaAs at the distance of several angstroems from

the graphene sheet, versus the contribution made by intrinsic deformation acoustical (DA) phonons of monolayer graphene. It has been shown that electron-PA phonon scattering is the dominant mechanism, limiting the mobility in graphene at relatively low carrier densities (*cf.* Fig. 8). Moreover, PA phonons change qualitatively the mobility dependence on the density of electrons and on the lattice temperature, respectively, in the regimes of high and low temperatures. In the high temperature (T) regime the momentum relaxation rate exhibits the same linear dependence on T but different dependences on the carrier density n—the mobility is inversely proportional to the density n and to the square-root of n, respectively for the DA and PA scattering mechanisms. In the low T Bloch-Gruneisen regime, the mobility shows the same square-root density dependence, but different temperature dependences—it is inversely proportional to the cube and fourth power of T, respectively for PA and DA phonon scattering (*cf.* Fig. 9).

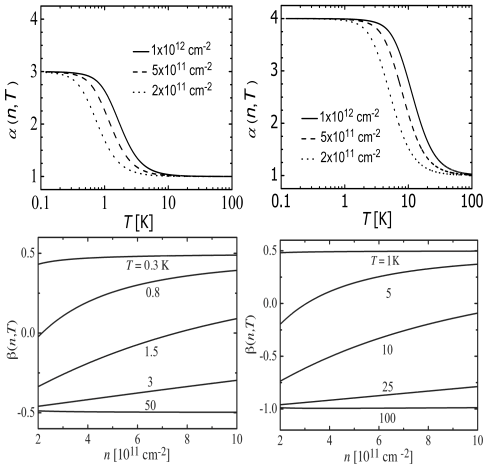

FIG. 8. The exponents $\alpha(n;T)$ (top panels) and $\beta(n;T)$ (bottom panels) describing the mobility behavior versus, respectively, temperature and the carrier density. The panels on the left and right hand sides depict, respectively, the PA and DA phonon limited mobilities.

Our prediction of this novel momentum relaxation channel, governed by the piezoelectric potential of the GaAs substrate, should influence the experimental findings on graphene device structures and be of general interest because of its importance for studying the underlying problem of carrier transport in graphene.

III. References

1. T. Ando, A. Fowler, and F. Stern, Rev. Mod. Phys. **54**, 437 (1982).
2. D. Awschalom and N. Samarth, Physics **2**, 50 (2009).
3. J. Fabian, A. Matos-Abiague, C. Ertler, P. Stano, and I. Žutič, Acta Phys. Slov. **57**, 565 (2007).
4. D. D. Awschalom and M. E. Flatte´, Nature Phys. **3**, 153 (2007).
5. S. A. Wolf, D. D. Awschalom, R. A. Buhrman, J. M. Daughton, S. von Molnár, M. L. Roukes, A. Y. Chtchelkanova, and D. M. Treger, Science **294**, 1488 (2001).
6. A. K. Geim, Science **324**, 1530 (2009).
7. K. S. Novoselov, A. K. Geim, S. V. Morozov, D. Jiang, Y. Zhang, S. V. Dubonos, I. V. Grigorieva, and A. A. Firsov, Science, **306**, 666 (2004).
8. K. S. Novoselov, A.K. Geim, S. V. Morozov, D. Jiang, M. I. Katsnelson, I. V. Grigorieva, S. V. Dubonos and A. A. Firsov, Nature, **438** 197 (2005).

9. A. H. Castro Neto, F. Guinea, N. M. R. Peres, K. S. Novoselov & A. K. Geim, Rev. Mod. Phys. **81**, 109 (2009); D. R. Cooper, B. D'Anjou, N. Ghattamaneni, B. Harack, M. Hilke, A. Horth, N. Majlis, M. Massicotte, L. Vandsburger, E. Whiteway, and V. Yu, ISRN Condensed Matter Physics, 2012, Article ID **501686**; V. N. Kotov, B. Uchoa, V. M. Pereira, F. Guinea, and A. H. Castro Neto, Rev. Mod. Phys. **84**, 1067 (2011).
10. A. K. Geim and K. S. Novoselov, Nature Mat. 6, 183 (2007); A. K. Geim and A. H. MacDonald, Phys. Today **60**(8), 35 (2007); S. K. Novoselov, Rev. Mod. Phys. **83**, 837 (2011).
11. **S. M. Badalyan,** A. Matos-Abiague, G. Vignale, and J. Fabian, Beating of Friedel oscillations induced by spin-orbit interaction, Phys. Rev. B **81**, 205314 (2010).
12. **S. M. Badalyan** and G. Vignale**,** Spin Hall drag in electronic bilayers, Phys. Rev. Lett., **103**, 196601 (2009).
13. M. M. Glazov, M. A. Semina, **S. M. Badalyan**, and G. Vignale, Spin accumulation from interlayer scattering in semiconductor bilayers, Phys. Rev. B **84**, 033305 (2011).
14. C. P. Weber, N. Gedik, J. E. Moore, J. Orenstein, J. Stephens, and D. D. Awschalom, Nature (London) **437**, 1330 (2005).
15. **S. M. Badalyan**, G. Vignale, and C. S. Kim, Finite width and local field corrections to spin Coulomb drag in a quasi-two-dimensional electron gas, Phys. Rev. Lett., **100**, 016603 (2008).
16. **S. M. Badalyan,** A. Matos-Abiague, G. Vignale, and J. Fabian, Spin-orbit interaction induced anisotropy of the plasmon spectrum, Phys. Rev. B **79**, 205305 (2009).
17. **S. M. Badalyan** and J. Fabian, Spin edge helices in a perpendicular magnetic field, Phys. Rev. Lett. **105**, 186601 (2010).
18. V. L. Grigoryan, A. Matos-Abiague**,** and **S. M. Badalyan,** Spin edge states: An exact solution and oscillations of the spin current, Phys. Rev. B **80**, 165320 (2009).
19. C. H. Park, F. Giustino, M. L. Cohen, and S. G. Louie, Phys. Rev. Lett. **99**, 086804 (2007).
20. M. Calandra and F. Mauri, Phys. Rev. B **76**, 205411 (2007).
21. W. K. Tse and S. Das Sarma, Phys. Rev. Lett. **99**, 236802 (2007).
22. T. Ando, J. Phys. Soc. Jpn. **76**, 024712 (2007).
23. S. M. Badalyan and F. M. Peeters, Phys. Rev. B **85**, 205453 (2012).
24. M. O. Goerbig, J.-N. Fuchs, K. Kechedzhi, and V. I. Fal'ko, Phys. Rev. Lett. **99**, 087402 (2007).
25. C. Faugeras, M. Amado, P. Kossacki, M. Orlita, M. Kuhne, A. A. L. Nicolet, Yu. I. Latyshev, and M. Potemski, Phys. Rev. Lett. **107**, 036807 (2011).
26. S. M. Badalyan and F. M. Peeters, Phys. Rev. Lett., in press.
27. A. Bostwick, F. Speck, T. Seyller, K. Horn, M. Polini, R. Asgari, A. H. MacDonald, and E. Rotenberg, Science **328**, 999 (2010).
28. A. Principi, M. Polini, and G. Vignale, Phys. Rev. B **80**, 075418 (2009).
29. B. Wunsch, T. Stauber, F. Sols, and F. Guinea, New J. Phys. **8**, 318 (2006).
30. E. H. Hwang and S. Das Sarma, Phys. Rev. B **75**, 205418 (2007).
31. Y. Barlas, T. Pereg-Barnea, M. Polini, R. Asgari, and A. H. MacDonald, Phys. Rev. Lett. **98**, 236601 (2007).
32. S. Das Sarma and E. H. Hwang, Phys. Rev. Lett. **102**, 206412 (2009).
33. S. H. Abedinpour, G. Vignale, A. Principi, M. Polini, W.-K. Tse and A. H. MacDonald, Phys. Rev. B **84**, 045429 (2011).

34. M. Polini, R. Asgari, G. Borghi, Y. Barlas, T. Pereg-Barnea, and A. H. MacDonald, Phys. Rev. B **77**, 081411(R) (2008).
35. M. Jablan, M. Soljacic, and H. Buljan, Phys. Rev. B **83**, 161409(R) (2011).
36. H. Schmidt, T. Ludtke, P. Barthold, E. McCann, V. I. Falko, and R. J. Haug, Appl. Phys. Lett. **93**, 172108 (2008).
37. S. Kim, I. Jo, J. Nah, Z. Yao, S. K. Banerjee, and E. Tutuc, Phys. Rev. B **83**, 161401(R) (2011).
38. L. A. Ponomarenko, A. A. Zhukov, R. Jalil, S. V. Morozov, K. S. Novoselov, V. V. Cheianov, V. I. Falko, K. Watanabe, T. Taniguchi, A. K. Geim, and R. V. Gorbachev, Nature Physics, **7**, 958 (2011).
39. S. Kim, I. Jo, D. C. Dillen, D. A. Ferrer, B. Fallahazad, Z. Yao, S. K. Banerjee, and E. Tutuc, Phys. Rev. Lett. **108**, 116404 (2012).
40. L. Britnell, R. V. Gorbachev, R. Jalil, B. D. Belle, F. Schedin, A. Mishchenko, T. Georgiou, M.I. Katsnelson, L. Eaves, S. V. Morozov, N.M.R. Peres, J. Leist, A.K. Geim, K.S. Novoselov, and L. A. Ponomarenko, Science **335**, 947 (2012).
41. R. V. Gorbachev, A. K. Geim, M. I. Katsnelson, K. S. Novoselov, T. Tudorovskiy, I. V. Grigorieva, A. H. MacDonald, S. V. Morozov, K.Watanabe, T. Taniguchi, and L. A. Ponomarenko, Nature Physics, DOI: 10.1038/**NPHYS2441**, (2012).
42. E. H. Hwang and S. Das Sarma, Phys. Rev. B **80**, 205405 (2009).
43. T. Stauber and G. Gomez-Santos, Phys. Rev. B **85**, 075410 (2012).
44. R. E. V. Profumo, R. Asgari, M. Polini, and A. H. MacDonald, Phys. Rev. B **85**, 085443 (2012).
45. S. M. Badalyan and F. M. Peeters, Phys. Rev. B **85**, 195444 (2012).
46. W.-K. Tse, Ben Y.-K. Hu, and S. Das Sarma, Phys. Rev. B **76**, 081401(R) (2007).
47. B.N. Narozhny, Phys. Rev. B **76**, 153409 (2007).
48. N. M. R. Peres, J. M. B. Lopes dos Santos, and A. H. Castro Neto, Europhysics Letters, **95**, 18001 (2011).
49. M. I. Katsnelson, Phys. Rev. B **84**, 041407(R) (2011).
50. E. H. Hwang, R. Sensarma, and S. Das Sarma, Phys. Rev. B **84**, 245441 (2011).
51. B. N. Narozhny, M. Titov, I. V. Gornyi, and P. M. Ostrovsky, Phys. Rev. B **85**, 195421 (2012).
52. M. Carrega, T. Tudorovskiy, A. Principi, M. I. Katsnelson, and M. Polini, New J. Phys. **14**, 063033 (2012).
53. B. Scharf and A. Matos-Abiague, Phys. Rev. B **86**, 115425 (2012).
54. S. M. Badalyan and F. M. Peeters, Phys. Rev. B **86**, 121405(R) (2012).
55. A. Pound, J. P. Carbotte and E. J. Nicol, EPL **94** 57006 (2011); Phys. Rev. B **84**, 085125 (2011).
56. F. Ding, H. Ji, Y. Chen, A. Herklotz, K. Dorr, Y. Mei, A. Rastelli, O. Schmidt, Nano Lett., **10**, 3453 (2010).
57. M. Woszczyna, M. Friedemann, M. Gtz, E. Pesel, K. Pierz, T. Weimann, F. J. Ahlers, Applied Physics Letters **100**, 164106 (2012).